[11]Helfrich, Ref. 5, has suggested, on purely phenomenological grounds, a relation between $\tan^2\theta$ and the degree of order $S$ which has some similarity to Eq. (8).

[12]S. Chandrasekhar and N. V. Madhusudhana, Acta Crystallogr., Sect. A 27, 303 (1971).

[13]P. Pieranski and E. Guyon, Phys. Rev. Lett. 32, 924 (1974).

[14]N. A. Clark, Phys. Lett. 46A, 171 (1973).

# Temporal Correlations near the Convection-Instability Threshold*

Wallace Arden Smith
*Department of Physics, City College of the City University of New York, New York, New York 10031*
(Received 21 February 1974)

I analyze Graham's theory of the threshold region of the convection instability in a fluid layer heated from below. I consider the situation where vertical boundary walls insure that a single spatial mode dominates in the threshold region. Equilibrium properties and the temporal correlation times for both the amplitude and intensity of that mode are presented.

In an incisive analysis,[1] Graham has introduced a generalized thermodynamic potential which governs the stability, the dynamics, and the fluctuations in a fluid layer heated from below near the onset of convection. Graham's formulation incorporates both fluctuating forces and the relevant nonlinearities of the hydrodynamic equations to describe the appearance of finite-amplitude convection at the Bénard point. With this theory we can understand the detailed dynamics of fluids for Rayleigh numbers in the immediate neighborhood of the critical Rayleigh number which marks the abrupt appearance of convection in the linear theory.[2] In this note I apply Graham's theory to the experimentally realistic situation of convection in a fluid layer enclosed by rigid vertical walls. I present detailed results on the equilibrium and dynamic behavior of the fluid throughout the convection threshold region.

For experimentally realizable convection cavities, the horizontal dimensions are much smaller than the correlation length of fluctuations near the Bénard point. Thus the rotational and translational symmetry in the fluid plane is effectively broken. To analyze the spatial dependence of the fluid flow one must then calculate the normal modes for the particular geometry of the convection cavity.[3] While the details of such a calculation are indeed complex, the general features are clear. For example, in a rectangular cavity, rolls parallel to the short wall with a wavelength near the critical wavelength (for the infinite-layer problem) suffer the least damping. Thus by properly choosing the dimensions of the experimental cavity, one can insure that *one* normal mode dominates in the threshold region. It is just this one-mode case I investigate.

With the spatial dependence of the convection determined from the normal-mode analysis, only the amplitude, $w$, of that normal mode remains as a fluctuating quantity. Thus Graham's functional Fokker-Planck equation reduces to an ordinary Fokker-Planck equation[4] for the probability density, $W(w)$, of that one stochastic variable:

$$\frac{\partial W}{\partial t} = -LW = \frac{\partial}{\partial w}\left(\frac{\partial \Phi}{\partial w} W + \frac{\partial W}{\partial w}\right), \tag{1}$$

where $\Phi = w^4/4 - aw^2/2$; $w$ measures the amplitude of the flow in units[5] such that the vertical component of the fluid velocity is $v_z(x,y,z) = wv_0 \times \Psi(x,y,z)$, with $v_0 = (9Q/4rVP^2)^{1/4}(\nu/l)$;

$$a = [a_0]\epsilon = [(9\pi^2/2P)(V/Qr)^{1/2}](R - R_c)/R_c$$

measures the deviation from the critical Rayleigh number; $t$ measures the time in multiples of $[3(V/Qr)^{1/2}(1+P)/P](l^2/\nu)$; $\Psi(x,y,z)$ gives the spatial dependence of the relevant normal mode and is normalized so that $\int \Psi(x,y,z)^2\, dV/V = 1$; and $r = \int \Psi(x,y,z)^4\, dV/V \simeq 2$ is the only quantity which depends on the details of the normal mode (the integrals extend over the entire convection cavity volume, $V$).

The equilibrium solution to the Fokker-Planck equation is

$$W_0(w) = N \exp(-\Phi) = N \exp(-w^4/4 + aw^2/2), \tag{2}$$

where $N$ normalizes the integral of $W_0$ over all $w$ to unity. The mean intensity $\langle I \rangle$ ($I = w^2$), the size of its fluctuations, $\langle \Delta I^2 \rangle$ ($\Delta I = I - \langle I \rangle$), and the

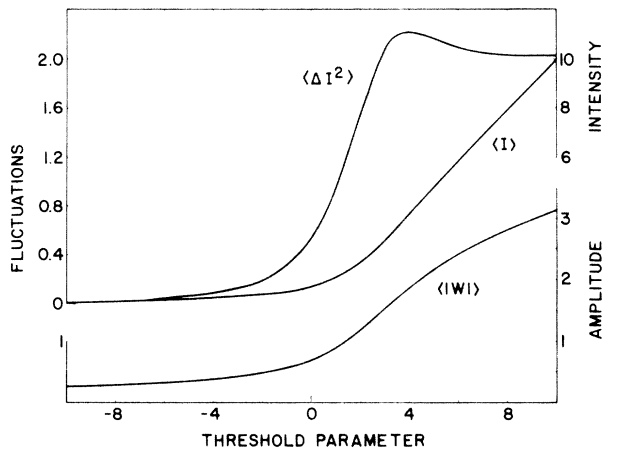


FIG. 1. Equilibrium properties as a function of threshold parameter $a$: mean intensity, $\langle I\rangle = \langle w^2\rangle$ (upper right-hand scale—five times the upper left-hand scale); mean absolute amplitude, $\langle |w|\rangle$ (lower right-hand scale); and intensity fluctuations, $\langle \Delta I^2\rangle$ (upper left-hand scale).

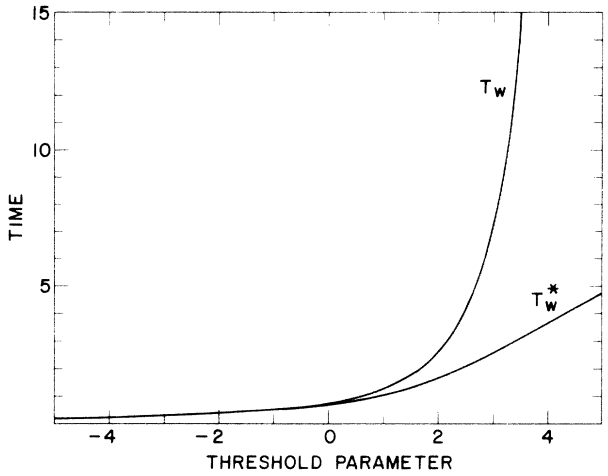


FIG. 2. Amplitude fluctuation times as a function of threshold parameter $a$. $T_w$ is the correlation time. $T_w{}^*$ measures the initial slope of the correlation function.

mean absolute amplitude $\langle |w|\rangle$ can be determined from $W_0$ by direct integration. Their values in the threshold region are given in Fig. 1. The approximations $\langle I\rangle = -1/a$, $\langle \Delta I^2\rangle = 2/a^2$, and $\langle |w|\rangle = 1/(-a)^{1/2}$ are valid far below the convection threshold ($a \ll 0$). Far above threshold ($a \gg 0$), $\langle I\rangle = a$, $\langle \Delta I^2\rangle = 2$, and $\langle |w|\rangle = a^{1/2}$ become valid approximations.

The temporal correlations in the fluctuations can also be calculated from equilibrium averages.[6] The initial derivatives of the correlation function $\langle w(t)w(0)\rangle$ can be expressed in terms of equilibrium averages,[7]

$$[d^n\langle w(t)w(0)\rangle/dt^n]_{(t=0)} = \int dw\, w(-L)^n w W_0(w), \quad (3)$$

where $L$, the differential operator given in Eq. (1), acts on everything to its right and the integration extends from minus to plus infinity. Since these initial derivatives form a Stieltjes series, one can approximate the correlation functions as a finite sum of exponentials (chosen so that the initial derivatives of the sum match the exact initial derivatives); one obtains thereby rigorous upper and lower bounds to the correlation function to any desired degree of precision. The efficacy of such an analysis has been noted[6]; a more detailed discussion will be presented elsewhere. A similar analysis applies to the intensity fluctuation correlation function, $\langle \Delta I(t)\Delta I(0)\rangle$.

The correlation time for amplitude fluctuations,

$$T_w = \int_0^\infty \langle w(t)w(0)\rangle\, dt/\langle I\rangle,$$

is directly proportional to $\langle I\rangle$ far below threshold and grows like[8]

$$\int_0^\infty dx \int_0^x dy \exp[(y^4 - x^4)/4 - a(y^2 - x^2)/2] \simeq \pi \exp(a^2/4)/2^{1/2}a$$

far above threshold. Its behavior in the threshold region is given in Fig. 2. The time scale determined by the initial slope of the correlation function,

$$T_w{}^* = -\langle I\rangle/[d\langle w(t)w(0)\rangle/dt]_{(t=0)},$$

is exactly proportional to $\langle I\rangle$. We get a more intuitive grasp of the difference between $T_w$ and $T_w{}^*$ if we view the decay of the correlation function as consisting of two stages. First $\langle w(t)w(0)\rangle$ decays to $\langle |w|\rangle^2$ on the time scale it takes for the random variable to move toward a local minimum of the potential $\Phi$. Next the correlation function decays to zero on the time scale that $w$ fluctuates to $-w$. $T_w{}^*$ is sensitive to the first of these stages, while $T_w$ reflects both. Below threshold, there is only one minumum of $\Phi$ at $w = 0$, and the time scales of both states are comparable: Thus $T_w$ and $T_w{}^*$ are coincident. Above threshold there are two minima of the potential $\Phi$ at $w = \pm a^{1/2}$. $T_w{}^*$ reflects the comparatively short time necessary for $w$ to reach a local minimum, while $T_w$ is dominated by the very long time needed for jumps over the large potential barrier between $w \simeq +a^{1/2}$ and $w \simeq -a^{1/2}$ (the time between spontaneous reversals in the sense of

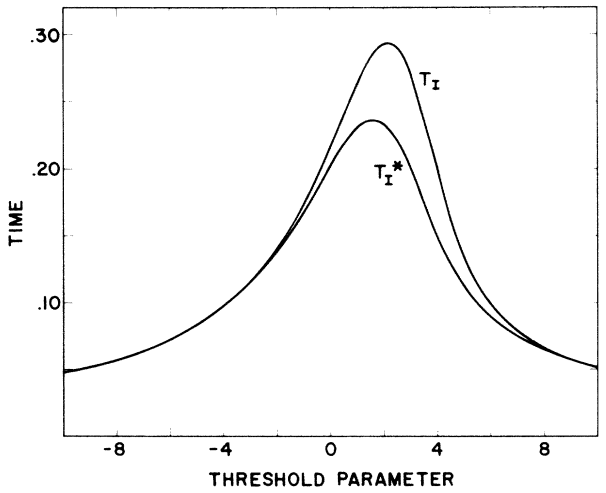


FIG. 3. Intensity fluctuation times as a function of threshold parameter $a$. $T_I$ is the correlation time. $T_I^*$ measures the initial slope of the correlation function.

rotation in the rolls).

The correlation time for intensity fluctuations,

$$T_I = \int_0^\infty \langle \Delta I(t) \Delta I(0) \rangle \, dt / \langle \Delta I^2 \rangle,$$

is shown in Fig. 3 for the threshold region. Outside the threshold region, $1/|a|$ is a valid approximation. The time scale determined by the initial slope of the correlation function,

$$T_I^* = -\langle \Delta I^2 \rangle / [d\langle \Delta I(t) \Delta I(0) \rangle / dt]_{(t=0)},$$

is also shown in Fig. 3. The near equality of $T_I$ and $T_I^*$ indicates that the decay of the correlation function is well represented by a single exponential.

Many aspects of these results reinforce the analogy between the appearance of a dissipative structure[9] (the convection cells) in this system far from thermal equilibrium and the onset of a phase transition in systems in thermal equilibrium. The fluctuations grow rapidly and slow down (see Figs. 1 and 3) as threshold is approached. A symmetry breaking also occurs at threshold. The large magnitude of $T_w$ above threshold reveals that the microscopic symmetry between positive and negative $w$ (the sense of rotation in the rolls) is effectively broken on a macroscopic scale. Moreover, since the size of the transition region is exceedingly small by macroscopic standards, the dissipative structure, like a phase transition, appears abruptly at the critical Rayleigh number.

The physical size of the effects described above is determined by the scale parameters $v_0$, $t_0$, and $a_0$ [defined following Eq. (1)]. The magnitude of the convection velocity is given by $v_0$, while $t_0$ gives the time scale of the fluctuations. The value of $a_0^{-1}$ gives the size of the threshold region in terms of $\epsilon$, the fractional deviation of the Rayleigh number from the critical Rayleigh number. Thus $a_0^{-1}$ determines how precisely one must regulate the thermal gradient to investigate the threshold region. For acetone at 20°C, in a cavity 1 mm thick and 25 mm$^3$ in volume,[5] one obtains $v_0 = 1.4 \times 10^{-4}$ cm/sec; $t_0 = 1.2 \times 10^4$ sec; and $a_0^{-1} = 6.6 \times 10^{-6}$. These values are typical of normal fluids and suggest that a detailed experimental investigation of the threshold region is a demanding task. Nevertheless, a clever experimenter may find a way to reveal these interesting phenomena.

It is a pleasure for me to acknowledge my debt to Robert Graham both for sending me the results of his research prior to publication and for subsequent illuminating correspondence. I am also grateful to J. B. Lastovka for many valuable discussions of the Bénard problem and, in particular, for discussions of his experiments on the Bénard instability. I am indebted to Bell Telephone Laboratories, Murray Hill, for their kind hospitality for a portion of the time during which this research was done. I wish to thank, in particular, Andrew D. Hall, Jr., for insights into the algebraic computer calculations using ALTRAN.

*Work supported in part by the U.S. Office of Naval Research and the U.S. Army Research Office (Durham).

[1]R. Graham, Phys. Rev. Lett. 31, 1479 (1973).

[2]See, for example, S. Chandrasekhar, *Hydrodynamic and Hydromagnetic Stability* (Oxford Univ. Press, London, 1961).

[3]See, for example, S. H. Davis, J. Fluid Mech. 30, 465 (1967). Far above threshold, the nonlinearities in the hydrodynamic equations alter, of course, the flow pattern from that given by the normal-mode analysis of the linear equations. In the threshold region, the principal effect of the nonlinearities is to limit the amplitude of the flow. In any case our analysis is not predicated on the exact nature of the normal-mode analysis. We only require that some single normal-mode describe the spatial dependence of the flow pattern; the validity of this hypothesis is an experimental fact.

[4]This Fokker-Planck equation differs from the laser Fokker-Planck equation in that the stochastic variable $w$ is a single real number in the range minus to plus infinity. The analog of the laser phase symmetry (invariance under translations in the plane of the fluid layer) is destroyed by the presence of the vertical walls. For a discussion of the laser Fokker-Planck equation

see, for example, H. Risken, in *Progress in Optics*, edited by E. Wolf (North-Holland, Amsterdam, 1970), Vol. 8.

[5]We use the same notation as Graham, except that we have altered the scales of $w$ and $t$ as noted in the text. We also characterize the deviation from threshold by $a$, which differs from Graham's $\epsilon$. We repeat Graham's notation for the reader's convenience: Rayleigh number $R=g\beta\Delta T l^3/\nu\kappa$; Prandtl number $P=\nu/\kappa$; $Q=\pi^2(Q_1+Q_2)/(1+P)$; $Q_1=g\beta kT/\rho C_p\nu^2\Delta T$; $Q_2=kT/\rho\nu^2 l$; $l$ and $V$, thickness and volume of the convection cavity; $\Delta T$, externally maintained temperature difference between the top and bottom of the convection cavity; $T$, average fluid temperature; (the following fluid properties have their value for acetone at 20°C given in parentheses) $\rho$, density (0.79 gm/cm$^3$); $C_p$, specific heat (2.18 J/g mC deg); $\beta$, volume expansion coefficient (0.0015/C deg); $\kappa$, thermometric conductivity ($1.04\times10^{-3}$ cm$^2$/sec); and $\nu$, kinematic viscosity ($4.11\times10^{-3}$ cm$^2$/sec). The acceleration of gravity is $g$ and Boltzmann's constant is $k$.

[6]W. A. Smith, Phys. Rev. Lett. 32, 1 (1974).

[7]The evaluation of these initial derivatives was greatly facilitated by performing algebraic manipulations on a computer using the ALTRAN language. See A. D. Hall, Commun. Assoc. Comput. Mach. 14, 517 (1971).

[8]R. Graham, private communication. This is an expression for the spontaneous reversal time.

[9]See, for example, P. Glansdorff and I. Prigogine, *Thermodynamic Theory of Structure, Stability, and Fluctuations* (Interscience, New York, 1971).

# Neutron-Scattering Study of the Momentum Distribution of $^4$He†

H. A. Mook
*Solid State Division, Oak Ridge National Laboratory, Oak Ridge, Tennessee 37830*
(Received 19 February 1974)

Neutron inelastic scattering at a momentum transfer of about 15 Å$^{-1}$ has been used to measure the scattering law $S(Q,\omega)$ with high accuracy for $^4$He at 1.2 and 4.2°K. At this momentum transfer the impulse approximation is nearly valid and momentum distributions for $^4$He can be determined directly from the data. The momentum distributions for the two temperatures show features not previously observed and provide new information to compare with theoretical results.

When neutrons are scattered with a sufficiently high momentum transfer $Q$ from a material, the scattering may be thought of as taking place from individual atoms and collective effects have little importance. For most materials the value of the momentum transfer $Q$ needed to be in the single-particle regime is prohibitively high; however for liquid $^4$He, a material of extreme interest, the value of $Q$ necessary is about 15 Å$^{-1}$, making experiments difficult but possible with neutrons available from a reactor.[1-7] Two prior experiments have been performed on $^4$He with momentum transfers of this magnitude, the first by Harling[8] with a time-of-flight technique and the second by Mook, Scherm, and Wilkinson[9] with a triple-axis spectrometer. The $^4$He momentum distribution $n_p$ depends on the derivative of the scattering distribution and the experimental data must have high accuracy and resolution to obtain a satisfactory result for $n_p$. Harling's data were of sufficient accuracy to obtain bulk quantities such as the average kinetic energy for the helium atoms but were unsuitable for extracting detailed information like $n_p$. The Mook, Scherm, and Wilkinson experiment concentrated around the peak of the scattering distribution in order to observe Bose-Einstein condensation and was of high accuracy in this region. However the data in the tails and part of the sides of the scattering distribution were not of sufficient accuracy to produce a reliable $n_p$. The data presented in this paper are of sufficient quality for the entire scattering distribution that detailed information about $n_p$ is available for the first time.

$n_p$ has been determined for two temperatures, 4.2 and 1.2°K. Both distributions show surprising structure and give information about $^4$He that was not previously available. The 1.2° distribution exhibits a peak of 0.2 Å$^{-1}$ that is clearly indicative of Bose-Einstein condensation. The remainder of the distribution shows structure that has not been observed in previous calculations for $n_p$ and thus suggests that more refined theoretical work is necessary. The data at 4.2°K show a large hump at a momentum of 2.25 Å$^{-1}$ which is in the roton region of the excitation spectrum. If a connection is made between the excitation spectrum and $n_p$, one is led to the surprising conclusion that rotons persist as distinct excitations at temperatures up to twice the tran-